Mon. Not. R. Astron. Soc. **274**, 75–84 (1995)

Optical spectroscopy of the *ROSAT* X-ray brightest clusters – II

C. S. Crawford,[1] A. C. Edge,[1] A. C. Fabian,[1] S. W. Allen,[1] H. Böhringer,[2] H. Ebeling,[2] R. G.McMahon[1] and W. Voges[2]

[1] *Institute of Astronomy, Madingley Road, Cambridge CB3 0HA*
[2] *Max-Planck-Institut für Extraterrestrische Physik, D-85740 Garching, Germany*

Received 1994 November 22; in original form 1993 October 15

ABSTRACT

We report results from the second stage of an optical follow-up study aimed at determining new redshifts for clusters of galaxies selected from the *ROSAT* All-Sky Survey. We review the optical properties of all the clusters obtained so far in this programme, which comprises 71 clusters up to a redshift of 0.3. The fraction of central galaxies exhibiting optical line emission and an excess blue continum is 34 per cent, consistent with smaller, previous, X-ray samples. There is no trend for this fraction to increase with redshift, although we find a clear tendency for the strongest line emitters to have the bluest continua. The probability of the presence of line emission and an excess blue continuum is increased for those galaxies with associated radio sources, although the strength of these features does not appear to be related to the power of the radio emission.

Key words: surveys – galaxies: clusters: general – cooling flows – galaxies: elliptical and lenticular, cD – galaxies: stellar content – X-rays: galaxies.

1 INTRODUCTION

X-ray surveys offer the most efficient way to select clusters of galaxies, due to the strong concentration of the emission in the cluster core and the resulting freedom from projection effects that complicate optical searches for clusters (Abell 1958; Lucey 1983). An X-ray flux-limited sample of approximately 50 clusters compiled from previous all-sky surveys showed evidence for cluster evolution and also that the fraction of clusters with cooling flows is greater than 70 per cent (Edge et al. 1990; Edge, Stewart & Fabian 1992, hereafter ESF). The only other comparable X-ray sample of clusters is that from the *Einstein* Medium Sensitivity Survey (EMSS) (Gioia et al. 1990a; Stocke et al. 1991), which contains 100 clusters over a range of fluxes. The EMSS also shows strong evolution (Gioia et al. 1990b; Henry et al. 1992) and is inferred to contain a high fraction of cooling flows (Pesce et al. 1990; Donahue, Stocke & Gioia 1992).

The recent *ROSAT* All-Sky Survey (RASS) has greatly increased the depth and resolution of our view of the X-ray sky, and has detected more than 1000 clusters of galaxies (Ebeling et al. 1993). In an attempt to create a more manageable sample, we are pursuing a programme to identify all the brightest sources from the RASS (an unabsorbed 0.1–2.4 keV flux above 3.2×10^{-12} erg cm^{-2} s^{-1}) that are associated with clusters of galaxies in the Northern Hemisphere at high galactic latitude ($|b| > 20°$), hereafter the Brightest Cluster Sample (BCS). Almost 200 RASS sources above this flux limit are correlated with clusters in the Abell and Zwicky catalogues using the statistical approach outlined by Ebeling et al. (1993). Many of the Abell and Zwicky clusters found are at redshifts above 0.1, where the redshift completeness of optical samples is low. More than 75 per cent of these Abell and Zwicky sources are detected as extended (compared to a point source) by the automatic detection routine in the Standard Analysis Software System (SASS) (Voges et al. 1992), making X-ray extent a very efficient method of selecting clusters. Examining all RASS extended sources that are not identified with an optically catalogued cluster, we find 40–50 additional sources that are associated with an overdensity of galaxies on optical sky survey plates. Most of these extended X-ray sources are associated with nearby galaxies and groups. The vast majority of the clusters selected by this X-ray method are at moderately low galactic latitude ($|b| = 20°$–$35°$) where the optical catalogues are incomplete. A more detailed comparison of the X-ray-selected and optically selected clusters will be discussed in a later paper. The selection method outlined implies an overall incompleteness of approximately 5 per cent, i.e. the number of X-ray-selected clusters missed is about 10. (This last number is obtained by assuming that the extended fraction of 0.75 applies to clusters not in the optical catalogues.)

This paper is the second one detailing the redshifts and optical properties of both the new sources and those where the distance was previously unknown, and brings the total, both optically catalogued and non-optically catalogued, sample of approximately 240 clusters to a high level of redshift completeness (more than 90 per cent now have measured redshifts). The X-ray analysis to obtain more accurate fluxes will soon be complete, enabling a final compilation of BCS.

The previous paper in this programme (Allen et al. 1992, hereafter Paper I) gave the redshifts of 29 clusters. Approximately 40 per cent of the central galaxy spectra showed an excess blue continuum and strong optical line emission similar to that associated with nearby cooling flow galaxies. In particular, Paper I reported the discovery of Z3146, the most luminous emission-line central cluster galaxy with a redshift $z < 1$ and a massive cooling flow (Edge et al. 1994). We describe here the redshifts and spectra of a further 47 cluster galaxies. The overall sample of spectra (from this paper and Paper I) provides an important subset of the optical spectra of the central galaxies in the whole sample. Therefore we review their spectral properties to determine the frequency of optical emission lines and to test for any possible evolution of these properties.

A value for the Hubble constant of $H_0 = 50$ km s^{-1} Mpc^{-1} and a cosmological deceleration parameter of $q_0 = 0$ have been assumed throughout.

2 OBSERVATIONS AND REDUCTION

2.1 Target selection

The clusters for this paper were selected either from cross-correlation with optical cluster catalogues or by their X-ray properties and by the absence of any published redshift for the cluster. We refer to the X-ray-selected objects by their number in the RASS catalogue, e.g. RX J0439.0+0520. In order to maximize the use of the telescope, several low galactic latitude sources (e.g. Z1121, which is host to the radio source 3C 162) and southern clusters were included in the target list. Although these clusters will not be included in the final BCS, they are selected using the same criteria as the rest of the sample, and we present them for completeness.

From a cross-correlation of the catalogued optical position, the positions of the X-ray source and that of the brightest galaxy in the cluster, we determine that the brightest galaxy is within 1 arcmin of the X-ray position for 80 per cent of all the clusters. This fact, coupled with the close agreement between the velocity of the brightest galaxy and the cluster mean, implies that the redshift of the brightest galaxy within 1 arcmin of the X-ray position of a cluster will give a reliable determination of the cluster redshift. If the cluster has two equally bright galaxies in the core, it is necessary to obtain both their redshifts.

2.2 Optical observations, reduction and analysis

Optical spectra of target central cluster galaxies were taken during the nights of 1992 December 25–27, using the Faint Object Spectrograph on the 2.5-m Isaac Newton Telescope, La Palma. This instrument yields low-resolution spectra over a wide wavelength range, with dispersion of 10.7 Å pixel^{-1} in the first order (5000–10 500 Å), 5.4 Å pixel^{-1} in the second order (3500–5500 Å), and a spectral resolution of 1.5 pixel. Observations were made through a slit of width 1.6 arcsec and length 6 arcsec, using typical exposures of 1000 s and a slit generally oriented at the parallactic angle. Each target observation was followed by a short observation of a nearby F8 star to enable removal of atmospheric absorption features in the data reduction. Three or four observations of flux standards (EG76, EG162, EG24 and BD+17°4708) were made through the night, each with the slit opened up to 5 arcsec. Exposures of copper–argon arc lamps were made for wavelength calibration, and of the twilight sky to generate flat-fields. Weather conditions were variable, with cloud cover and humidity increasing sufficiently to prohibit observing from the middle of the third night. The seeing was on average ~1.7 arcsec. The data were reduced in an identical manner to those in Paper I, including corrections for Galactic reddening, and the redshift determinations used the same technique with new observations of both a K5 star and the central galaxy of A1795. Some of the more interesting spectra with emission lines are shown in Fig. 1.

10 additional spectra were taken using the Intermediate Dispersion Spectroscopic and Imaging System (ISIS) on the WHT during the nights of 1992 April 23 and October 3. The spectra are of moderate resolution (5 Å pixel^{-1}), covering 3800–8800 Å, and were taken in good seeing conditions (1.2 and 0.8 arcsec, respectively) with a 1.5-arcsec slit and exposures of 600 s. The flux standards HD 84937, HR 4468 and Wolf 1346 were observed with a 9-arcsec slit for calibration purposes. The four spectra obtained in April were not taken at the parallactic angle due to technical problems, affecting the observations of A971, A990, Z3916 and A1423. Calibration spectra of nearby F8 spectra were not taken for these objects, so no correction was made for atmospheric absorption bands. The redshifts were determined in the same way and using the same templates as the INT spectra.

3 RESULTS

3.1 Redshifts

We took spectra of 51 targets associated with 48 X-ray sources from the RASS. Where there were two dominant galaxies in the cluster, we took a spectrum of each galaxy. If any of the potential cluster identifications also had a stellar object as well-aligned (or better) with the SASS coordinates, we took its spectrum to check against the presence of an AGN. Two sources were clearly identified as broad-line active galaxies, and a third as a foreground star (bad weather precluded observation of further targets in this field). Whilst it is possible that cluster emission contributes to the X-ray source in the RASS, we have assumed that where an active galaxy is present, it dominates the RASS detection. One of the AGN is particularly interesting, as it is 5 arcmin from A2507, a cluster at $z = 0.196$ whose X-ray emission has been well studied from both *Ginga* and *HEAO-1* observations (Johnson et al. 1983; Arnaud et al. 1991). Our identification of a Balmer-line-dominated foreground AGN ($z = 0.066$) at the SASS position (RX J2256.6+0525) raises the possibility that the published X-ray spectra of A2507 may be con-

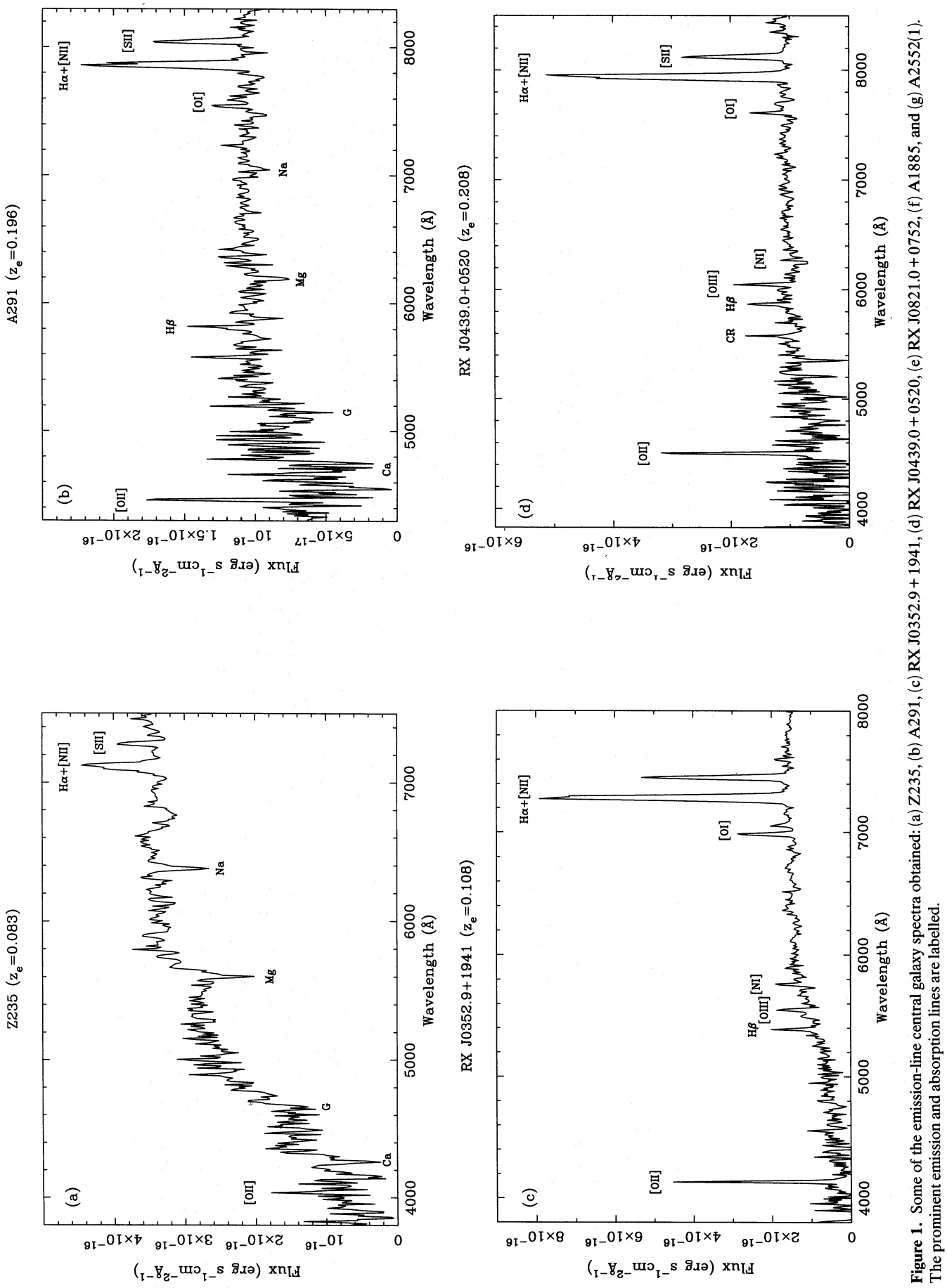

Figure 1. Some of the emission-line central galaxy spectra obtained: (a) Z235, (b) A291, (c) RX J0352.9 + 1941, (d) RX J0439.0 + 0520, (e) RX J0821.0 + 0752, (f) A1885, and (g) A2552(1). The prominent emission and absorption lines are labelled.

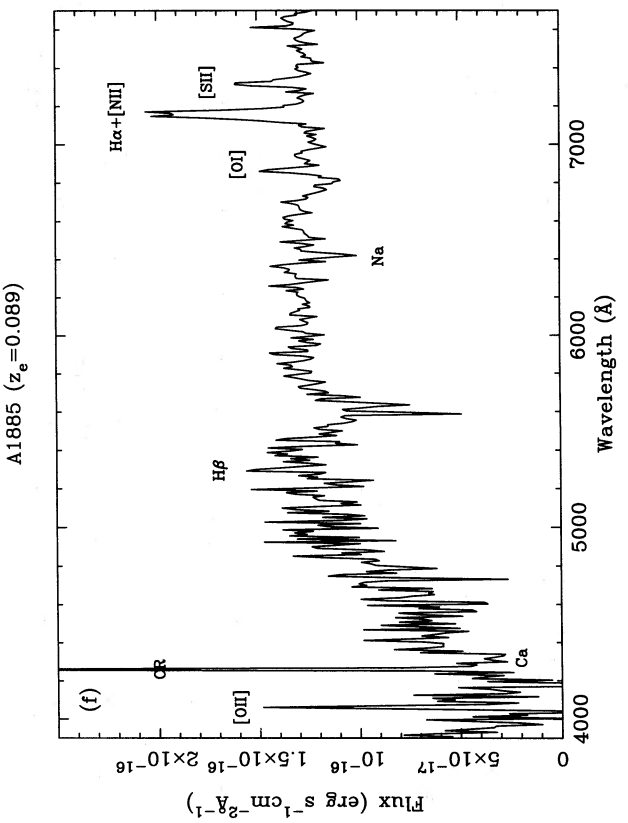

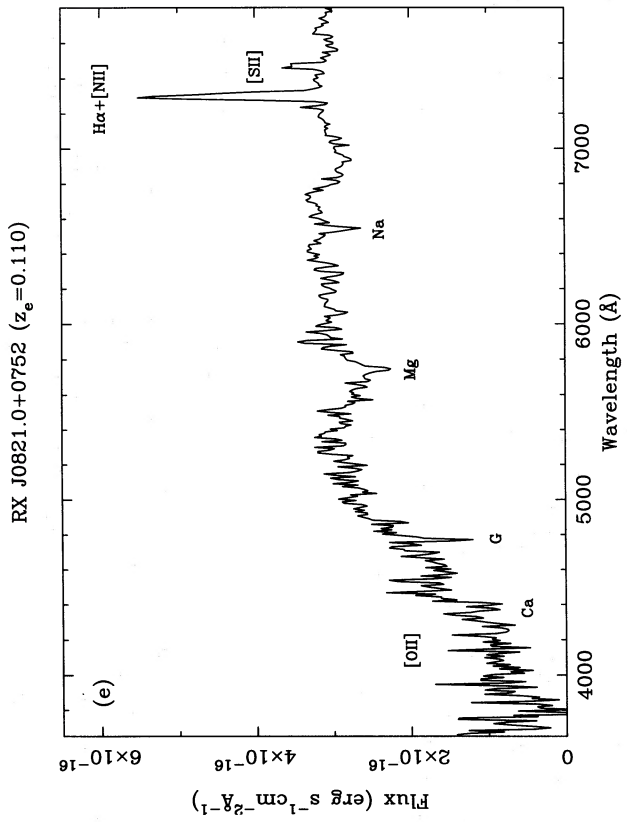

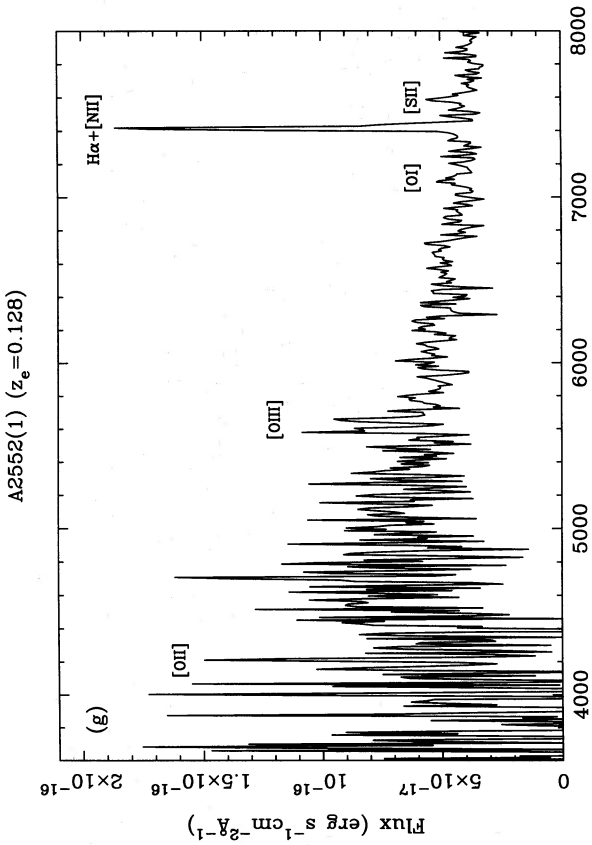

Figure 1 – *continued*

taminated by the AGN. This is being investigated in more detail using a pointed *ROSAT* observation and the *Ginga* spectrum (Elbaz et al., in preparation). The INT FOS spectrum is presented by Brandt et al. (1994). There is no radio or *IRAS* source at the position of the AGN.

There is one cluster (A689) for which the identification is ambiguous. The spectrum of the central galaxy of A689 is peculiar, showing only uncertain absorption features and a very blue continuum. Multicolour images (Edge, private communication) show that the galaxy has an unusually blue, unresolved core; there is a 40-mJy Green Bank 4.85-GHz survey source coincident with the galaxy, and the X-ray emission is not significantly extended. We therefore suggest that it is a candidate BL Lac object.

The redshift for A689 is given as provisional in Table 1 because of its poor signal-to-noise ratio. There are two other spectra of similarly poor quality [Z353 and A2552(2)] which are also marked as provisional redshifts, although the identification of the associated X-ray source as a cluster is clear as both are significantly extended.

Table 1. New redshifts. All are central dominant galaxies in clusters, apart from III Zw 054 (marked by a ‡) which is a galaxy. Where no equivalent width is given for Hα, this is because it coincided with sky absorption bands in the spectrum. The *ROSAT* identifier is given in the first column, and the optical position in the third and fourth columns. Note that the equivalent widths quoted are for Hα and not Hα + [N II] as used in Paper I.

ROSAT (2000)	Name	RA(1950)	DEC(1950)	z(e)	z(a)	$W_{H\alpha}$ (Å)	Radio Flux (1.4 GHz)
RX J0043.9+2424	Z235	00 41 12.7	24 07 56	0.083	0.083	4.0±1.0	111 mJy*
RX J0107.8+5408	Z353	01 04 40.8	53 50 32	—	†0.109	1.7±0.8	—
RX J0152.7+0100	A267	01 50 07.7	00 45 38	—	0.230	−1.1±1.04	—
RX J0201.7−0211	A291	01 59 10.7	−02 26 17	0.196	0.197	20.9±0.9	135 mJy
RX J0301.6+0155	Z808	02 59 03.0	01 43 27	0.170	0.169	2.6±0.9	500 mJy
RX J0303.4+0155	A409	03 00 45.8	01 43 50	—	0.153	0.1±0.8	—
RX J0341.3+1523	‡III Zw 054	03 38 28.9	15 14 10	—	0.029	0.6±0.6	—
RX J0352.9+1941		03 50 05.0	19 32 06	0.108	0.109	80.2±1.6	—
RX J0439.0+0520		04 36 22.7	05 14 51	0.208	—	55.9±1.5	513 mJy*
RX J0501.4−0332	A531	04 58 46.3	−03 38 09	—	0.094	−1.1±0.4	—
RX J0503.1+0608		05 00 26.4	06 03 44	—	0.088	−0.3±0.4	—
RX J0510.7−0801		05 08 23.4	−08 05 23	—	0.217	−0.1±0.8	—
RX J0631.4+2500	Z1121	06 28 19.2	25 03 10	—	0.083	1.8±0.6	988 mJy
RX J0638.1+4747	Z1133	06 34 17.4	47 50 31	—	0.174	−0.5±0.6	—
RX J0800.9+3603	A611	07 57 40.7	36 11 40	—	0.288	1.1±1.4	—
RX J0811.3+7002	A621	08 06 02.5	70 11 22	—	0.223	−2.2±1.0	135 mJy*
RX J0821.0+0752		08 18 21.0	08 01 21	0.110	0.110	17.2±0.8	—
RX J0828.1+4446	A667	08 24 38.7	44 55 59	—	0.145	0.0±0.5	—
RX J0837.4+1458	A689	08 34 36.8	15 08 52	—	†0.086	1.0±0.6	146 mJy*
RX J0842.9+3621	A697	08 39 46.2	36 32 48	—	0.282	3.2±1.4	—
RX J0910.6−1035	A761	09 08 17.9	−10 22 59	—	0.091	−0.5±0.6	—
RX J0917.9+5143	A773(1)	09 14 23.9	51 56 13	—	0.216	−0.1±0.8	—
	A773(2)	09 14 24.1	51 56 38	—	0.224	−0.5±0.5	—
RX J0952.8+5153	Z2701	09 49 29.8	52 07 12	0.214	0.215	3.4±0.8	—
RX J1000.5+4409(1)		09 57 18.7	44 23 38	0.153	0.155	2.7±2.5	—
RX J1000.5+4409(2)		09 57 24.5	44 23 08	0.153	0.153	2.8±0.9	—
RX J1020.0+4059	A971	10 16 53.3	41 14 24	—	0.093	−0.4±0.2	—
RX J1023.7+4908	A990	10 20 34.2	49 23 51	—	0.142	−0.4±0.7	—
RX J1114.3+5823	Z3916	11 11 25.5	58 39 42	0.206	0.204	7.1±0.7	—
RX J1157.3+3337	A1423	11 54 42.6	33 53 19	—	0.213	−0.1±0.6	29 mJy
RX J1205.2+3920		12 02 37.6	39 37 30	—	0.037	−1.0±0.4	—
RX J1257.5+6929	Z5604	12 55 30.9	69 46 37	—	0.227	−1.6±1.1	—
RX J1413.7+4339	A1885	14 11 45.0	43 53 43	0.089	0.090	10.9±1.0	173 mJy*
RX J1421.6+4932	Z6718	14 19 47.3	49 46 44	—	0.071	−2.1±0.8	—
RX J1421.7+3717	A1902	14 19 36.2	37 31 10	—	0.160	—	—
RX J1510.3+3332	A2034(1)	15 08 09.1	33 45 22	—	0.115	−0.6±0.7	—
	A2034(2)	15 08 10.6	33 40 32	—	0.111	0.4±0.8	—
RX J1627.0+5529	A2201	16 25 54.6	55 35 06	—	0.130	−0.1±0.5	—
RX J1717.8+1941	A2254	17 15 35.6	19 43 58	—	0.178	0.8±0.8	—
RX J1720.1+2740	A2259	17 18 10.4	27 43 06	—	0.164	—	—
RX J1722.4+3208	A2261	17 20 34.7	32 10 46	—	0.224	0.4±0.5	—
RX J1723.8+8553	A2294	17 37 01.7	85 55 17	0.178	—	51.7±3.2	—
RX J1757.1+5351	A2292	17 56 04.4	53 51 51	—	0.119	2.0±0.6	146 mJy*
RX J2311.6+0338	A2552(1)	23 08 58.2	03 21 34	0.128	—	70.0±2.4	—
	A2552(2)	23 09 00.4	03 21 46	†0.137	—	4.1±1.3	—
RX J2336.7+2355	A2627(1)	23 34 11.3	23 38 51	—	0.127	—	456 mJy
	A2627(2)	23 34 12.0	23 38 08	—	0.122	−0.5±0.5	—
RX J2337.6+0016	A2631	23 35 06.0	−00 00 21	—	0.278	−1.9±0.9	139 mJy

The redshifts marked by a † should be regarded as provisional due to poor signal-to-noise spectra.
Radio fluxes marked with an asterisk are extrapolated from 4.85 GHz, assuming a spectral index of −1.
The most likely central dominant galaxy in RX J1000.5 + 4409 is galaxy (1), and in A2034 it is galaxy (2).
In A773, A2552 and A2627 the two galaxies observed appear equally dominant.

The identification of a further source, A2552(1), remains ambiguous from its spectrum, which contains both narrow emission lines and an exceptionally blue continuum without absorption features. The power-law nature of the continuum suggests that it is better classified as an AGN. Optically this appears as one of two equally dominant central galaxies, and it has a redshift only 2400 km s^{-1} different from A2552(2). The spectrum of A2552(2) itself is poor, and its redshift relies on a single emission feature, and should be regarded as provisional.

Including A689, we obtain a total of 42 clusters with new redshifts. All the clusters are listed with their X-ray and optical positions, the redshift obtained by cross-correlation against absorption features (and from emission features, where possible) in Table 1. The redshifts have errors of ± 0.001. For completeness, we also include in Table 1 the redshift of an isolated galaxy identified from the RASS with a redshift determined from our observations (III Zw 054), but do not comment on it further.

Combining the new results with those in Paper I, we plot the total redshift distribution of the newly identified clusters in our sample so far (Fig. 2). The majority are located at redshifts between 0.1 and 0.15, which is consistent with most sources being associated with Abell or Zwicky clusters which are more remote than those usually studied. The most distant of these new objects remains Z3146, at a redshift of 0.291, from Paper I. The redshift cut-off reflects the limits of the optical survey plates and the smaller X-ray extents for more distant clusters, rather than any great decrease in the number of X-ray-luminous clusters at these redshifts. The identification of clusters beyond a redshift of 0.3 associated with X-ray sources will require independent CCD imaging or deeper photographic plates.

3.2 Optical line emission

Optical line emission is evident in 11 galaxies, principally from the lines of Hα and [N II]$\lambda\lambda$6548, 6584. The equivalent width of Hα is listed for each spectrum in Table 1 (although note that the fainter Hα systems are those that have stronger [N II] emission, and so the line emission is more significant than it appears from the equivalent width of Hα alone). The total incidence of line emission in the BCS central cluster galaxies so far is now 34 per cent. Distant central cluster galaxies with strong line emission have been *inferred* to be at the centre of cooling flows (Nesci et al. 1989; Donahue et al. 1992), but this has not been confirmed by direct X-ray imaging of the clusters. ESF determined the occurrence of both line emission and cooling flows in the 50 brightest clusters at low redshifts ($z < 0.1$), and found that 39 ± 9 per cent showed significant line emission. As the ESF sample contains 70–90 per cent cooling flows, it can be deduced that 35–70 per cent of the central galaxies in cooling flows show detectable optical line emission. Hence we find general agreement between the ESF sample, the *Einstein* Medium Sensitivity Survey (EMSS: Donahue et al. 1992) and our BCS. The only apparent exception to this agreement is the higher frequency of line emission in the highest redshift subsample ($z > 0.2$) of the EMSS (five out of nine, or 56 per cent), claimed by Donahue et al. (1992) as evidence for evolution in the fraction cooling flows. The same redshift band in the BCS shows an emission-line frequency of 35 per cent (seven in 20), and thus does not support any of the evolution claimed by Donahue et al. from a sample half the size. The higher frequency in the more distant EMSS clusters is well within the 90 per cent confidence limit expected from a sample of nine. Note that the quoted fraction of galaxies with emission lines is a function of the detection limit of the observations and the intrinsic line luminosity of each galaxy. Our detection limit and that of Donahue et al. (1992) are similar, so the fractions are comparable and correspond to an intrinsic luminosity of 3×10^{40} erg s^{-1} in Hα for the mean redshift. This effect does not introduce a significant redshift bias into the calculated fractions.

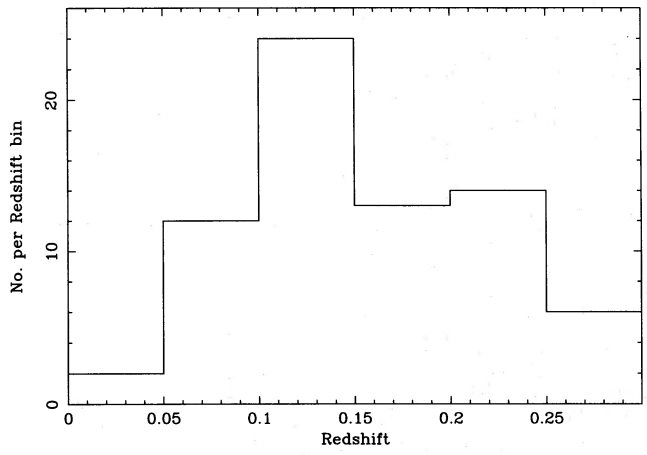

Figure 2. The redshift distribution of all the newly identified BCS clusters given here and in Paper I.

We have measured the fluxes of the principal emission lines using the same method described in Paper I, and they are summarized in Table 2. Where line emission was not significantly detected we have given the 2σ upper limit, except for those spectra which were too noisy to give any useful limit. None of the galaxies shows lines of comparable luminosity to the most extreme discovered in Paper I, typically spanning Hα luminosities of 3×10^{40}–8×10^{41} erg s^{-1}, with a single galaxy (that associated with RX J0439.0+0520) above 10^{42} erg s^{-1}. At lower redshifts, such emission-line nebulae are known to extend over regions typically 5–10 kpc in diameter, often in a patchy or filamentary form (Heckman 1981; Cowie et al. 1983; Hu, Cowie & Wang 1985; Johnstone, Fabian & Nulsen 1987; Heckman et al. 1989; Crawford & Fabian 1992). It is thus unlikely that our single slit observation will encompass the entire Hα luminosity associated with those systems at comparatively lower redshift (approximately $z < 0.1$). Without knowledge of the size of individual nebulae we cannot compensate for this effect, but note that we can expect our Hα luminosity of Z235, A1885, RX J0352.9+1941 and RX J0821.0+0752 (the lowest redshift emission-line systems) to be most affected, and that for these galaxies in particular the luminosity could be considered a lower limit. (The only emission-line object at comparable redshifts from Paper I is the observation of A1795 included for comparison.)

We combine these clusters with other new systems from Paper I to examine the relations between various properties of the emission lines. As originally pointed out by Heckman et al. (1989), there is a general trend for the more X-ray-luminous clusters to have lower ionization spectra and higher

Table 2. Line fluxes in units of 10^{-16} erg cm^{-2} s^{-1}. The FWHM is measured from the Hα and [N II] complex.

Name	Hα λ6563	Hβ λ4681	[NII] λ6584	[SII] λ6717	[OIII] λ5007	[OII] λ3727	[OI] λ6300	L(Hα) 10^{40} erg s^{-1}	FWHM km/s
Z808	3.9±0.9	<2.8	8.2±1.0	2.5±0.9	<2.8	<7.8	<0.5	5.7 ± 1.3	380±110
Z235	14.5±2.0	<7.2	25.2±2.1	9.2±2.6	<7.2	17.2±4.4	<2.3	4.7 ± 0.7	730±90
RX J0352.9+1941	139.8±2.7	20.9±2.2	128.9±2.4	78.0±3.1	17.8±2.3	67.8±7.1	33.8±2.0	78.0 ± 1.5	790±20
RX J0439.0+0520	72.2±2.0	18.0±2.1	106.7±2.0	40.4±2.2	20.4±2.2	58.0±7.0	12.7±1.6	164.0 ± 4.5	790±20
RX J0821.0+0752	60.0±2.8	<5.4	29.7±2.2	12.0±2.3	<2.0	7.3±2.6	<0.7	34.8 ± 1.6	730±60
A291	26.7±1.1	9.6±2.3	21.4±1.0	15.2±1.3	<3.6	23.5±5.3	6.1±1.0	53.9 ± 2.3	630±40
Z2701	5.7±1.8	<13.6	12.1±1.9	4.2±2.0	<4.8	<15.4	<2.2	13.8 ± 4.5	380±100
RX J1000.5+4409(1)	3.0±1.0	<3.4	7.2±1.1	<2.0	<3.2	<10.8	2.2±0.9	3.5 ± 1.2	480±140
RX J1000.5+4409(2)	2.9±0.9	—	4.1±1.1	<1.3	—	—	<1.9	3.4 ± 1.1	460±390
A1885	14.8±1.1	6.5±2.6	17.0±1.1	8.3±1.3	<4.6	19.5±4.5	5.1±1.0	5.5 ± 0.4	660±80
A2292	6.6±1.5	< 3.8	14.1±1.3	<1.9	< 3.5	<2.3	<2.0	4.5 ± 1.3	280±50
A2294	20.2±1.6	5.6±1.4	10.0±1.0	3.1±1.1	8.3±1.4	< 6.2	< 1.8	32.7 ± 1.6	185±20
Z3916	15.8±1.9	<4.6	17.6±1.9	11.9±1.8	<3.1	<8.6	—	35.1 ± 3.0	355±35

Hα luminosities. Heckman et al. broadly divided the cooling flow nebulae into class I systems – those with a high-ionization state and lower Hα luminosity – and class II – those Hα-luminous systems associated with stronger cooling flows and galaxies with powerful central radio sources. With our larger sample of the combined BCS we find no division into two classes on the basis of line intensity ratios, but the trend of ionization with cluster properties may be better regarded as a continuous distribution (Fig. 3). In Paper I, however, we noted two Hα-bright systems (A1068 and A2146) amongst those systems showing a high-ionization state. To these we now add the most Hα-luminous galaxy in our present data set, RX J0439.0+0520, which also shows [O II]λ3727/[O III]λ5007 < 3 and [N II] > Hα line ratio. The anomalous behaviour of these three galaxies is demonstrated in Fig. 4, where they stand out from the general trend in having a high [N II]/Hα for their large Hα luminosity. We find no correlation between either the Hα luminosity or the ionization state and the velocity width of the lines, as has been claimed by Crawford & Fabian (1992), but note that these FOS spectra probably lack sufficient spectral and spatial resolution to test this hypothesis.

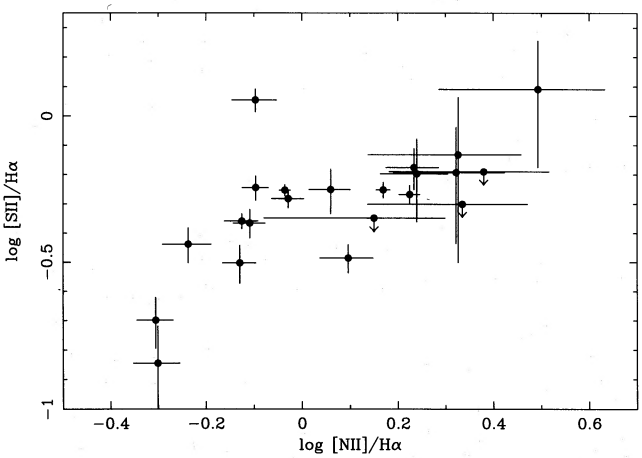

Figure 3. Line intensity ratio diagram of [N II]λ6584/Hα versus [S II]λ6717/Hα showing a continuous variation in ratios between the two extremes.

3.3 Excess blue light

As detailed by many authors, the majority of the strong emission-line galaxies show an excess blue continuum over that expected from a normal cD galaxy (Johnstone et al. 1987; Romanishin 1987; McNamara & O'Connell 1989, 1993). We have modelled this extra component using a simple spectral synthesis technique of fitting the data by a non-excess galaxy continuum in combination with a single main-sequence stellar spectrum. The template cD galaxy was created from the average of the rest-frame spectra of high signal-to-noise observations of RX J0341.3+1532, RX J0503.1+0608, NGC 7556 and A2627(2). Template stellar spectra were generated using the Kurucz (1979) model atmospheres. The emission lines were artificially removed from the galaxy spectra, which were then fitted typically over 3200–7500 Å in the rest-frame. In agreement with previous results (Paper I; Crawford & Fabian 1993), nearly all the data were well fitted by the combination of a B5 main-sequence spectrum with the template cD. The blue excess components of RX J1000.5+4409(2) and RX J0821.0+0752 were fitted marginally better by an A0 spectral type. Neither RX J0352.9+1941 nor Z235 required any blue light, but we note that RX J0352.9+1941 in particular was amongst those erroneously not observed at the parallactic angle. As

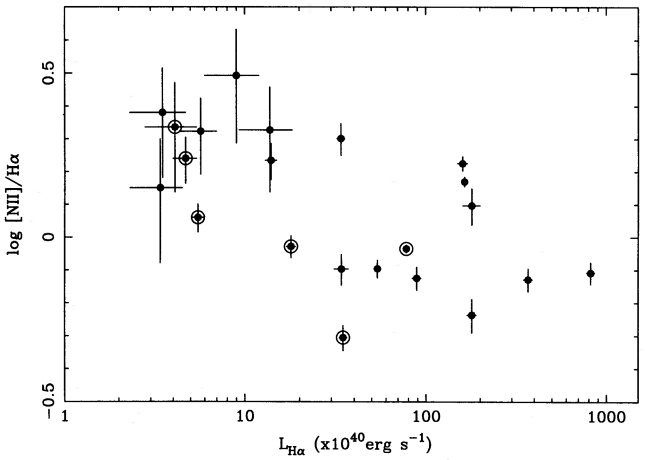

Figure 4. The variation of the ionization state of the gas (as described by the [N II]λ6584/Hα intensity ratio) with the observed Hα luminosity. Ringed points are those lower redshift galaxies where we expect that the measured Hα luminosity represents a lower limit to the actual value.

can be seen in Fig. 1, RX J0352.9+1941 has a noticeable lack of light in the second-order spectrum, falling well below even a standard elliptical galaxy continuum. This is not due to inadequate sky-subtraction, and so it represents a real loss of light from the slit.

We have also quantified the blue light using the δBR ratio of continuum light, defined in Paper I as

$$\delta BR = \frac{\int_{3500}^{3650} F_\lambda \delta\lambda}{\int_{5800}^{6200} F_\lambda \delta\lambda},$$

where the flux is integrated in the galaxy rest-frame. Table 3 lists the calculated values of δBR, with the fraction of blue continuum component obtained from the spectral synthesis modelling. In Fig. 5, we plot the variation of measured Hα luminosity against δBR. Although our present observations are mainly of the less Hα-luminous systems, we find that they continue the trend for the larger amounts of blue light to be associated with the more luminous, or class II, systems. Although the most line-luminous and bluest systems in the combined sample lie at high redshift, we do not find any obvious correlation between either δBR or the Hα luminosity with redshift.

3.4 X-ray data

The X-ray flux for inclusion in this sample is the same as in Paper I, namely 2×10^{-12} erg cm^{-2} s^{-1} (0.1–2.4 keV, unabsorbed). At this flux level the luminosity of the clusters at redshifts of 0.1 and 0.2 are 2×10^{44} and 8×10^{44} erg s^{-1}, respectively. We are pursuing a programme of follow-up pointed observations with *ROSAT* of clusters at redshifts above 0.1 from the Paper I sample, and find a high fraction of cooling flows (seven out of the eight observed so far). This rate of occurrence is in agreement with that seen at low redshift (ESF), where over 70 per cent of clusters contain cooling flows. The high percentage of cooling flows in this subsample of the BCS may be in part due to the susceptibility of X-ray-imaging surveys to miss low surface brightness, non-cooling flow clusters (Pesce et al. 1990). The strongest cooling flow observed so far ($1000\,M_\odot$ yr^{-1}) from the new BCS is in Z3146, which is both the most distant cluster in the sample and the most line-luminous (Edge et al. 1994).

3.5 Radio sources

On examination of radio surveys, all-sky (e.g. Gregory & Condon 1991; White & Becker 1992) and Abell cluster samples (e.g. Owen et al. 1982; Ball, Burns & Lokern 1993), there are 12 detections of radio sources within 1 arcmin of the brightest galaxy in the sample in this paper (Table 1), with a further four from Paper I. Only one of these detections (A1068; Ball et al. 1993) is less than 100 mJy at 1.4 GHz (or its equivalent assuming a radio spectral index of -1). This flux limit results in a sensitivity limit in log radio power at 1.4 GHz ($P_{1.4}$) of 24.6 W Hz^{-1} at a redshift of 0.1, 25.2 at a redshift of 0.2, and 25.5 a a redshift of 0.3. The mean log radio power of the detections is 25.0 with a detection rate of 13 per cent in total, 7 per cent $P_{1.4}>25$ and 5 per cent $P_{1.4}>25.5$. Given the number of clusters with redshifts above 0.2 with no radio detection, the fraction of detections with $P_{1.4}>25$ is a lower limit. To compare these detection rates with those for other samples, the detection rate for the ESF sample is 18 per cent for $P_{1.4}>25$ and 6 per cent for $P_{1.4}>25.5$, whilst the radio luminosity function of Abell cDs of Ball et al. (1993) implies a 25 per cent detection rate for $P_{1.4}>25$. Therefore the radio properties of the central galaxies in this subsample are consistent with other samples of central cluster galaxies when the poor limits at higher redshift are considered.

4 DISCUSSION

In the course of our redshift follow-up programme for *ROSAT* clusters we have amassed a sample of 80 spectra of central galaxies. Though not quite complete, the sample is three times larger than in previous studies of the frequency and nature of line-emitting gas at high redshift (Donahue et al. 1992). Optical follow-up is important not just for providing redshifts for calculations of X-ray luminosity and spatial correlation functions, but also for providing insight into the optical properties of the central cluster galaxies as a sample. As more distant X-ray-selected clusters are uncovered from the RASS and from deep pointed observations, we will be able to study not only the optical properties of individual central cluster galaxies, but also how these properties evolve with redshift.

The optical properties of the central cluster galaxies in the new clusters so far identified strongly resemble those seen in cooling flows at lower redshifts, in not only the fraction showing line emission but also in the line ratios, Hα luminosity and excess blue continuum. In particular, clusters selected by extended X-ray emission in the SASS analysis do not have properties any different from those identified from the optical catalogues of Zwicky and Abell. The lower redshift sources are either too poor to be classed as Abell richness 0, or are richness class 0 but overlooked by Abell. There is a substantial incompleteness in richness class 0 in the Abell catalogue (Ebeling et al. 1993; Lucey 1983). The higher red-

Table 3. Blue continuum components.

Name	F_{star}/F_{gal} (3500Å)	F_{star}/F_{gal} (4500Å)	Spectral Type	δBR	N_{stars}
Z235	<0.07	<0.01	B5	0.07	$< 7.3 \times 10^4$
A291	0.75	0.31	B5	0.27	7.8×10^6
Z808	0.48	0.13	B5	0.07	1.8×10^6
RX J0352.9+1941	<0.14	<0.02	B5	0.07	$< 5.8 \times 10^4$
RX J0439.0+0520	0.70	0.26	B5	0.20	4.7×10^6
RX J0821.0+0752	0.32	0.14	A0	0.10	1.1×10^7
Z2701	0.73	0.29	B5	0.16	7.4×10^6
RX J1000.5+4409(1)	0.73	0.30	B5	0.14	2.4×10^6
RX J1000.5+4409(2)	0.58	0.33	A0	0.17	1.1×10^7
A1885	0.42	0.10	B5	0.04	4.4×10^5
A2292	<0.03	<0.01	B5	0.06	$< 3.1 \times 10^5$
Z3916	<0.04	<0.01	B5	0.04	$< 1.1 \times 10^5$

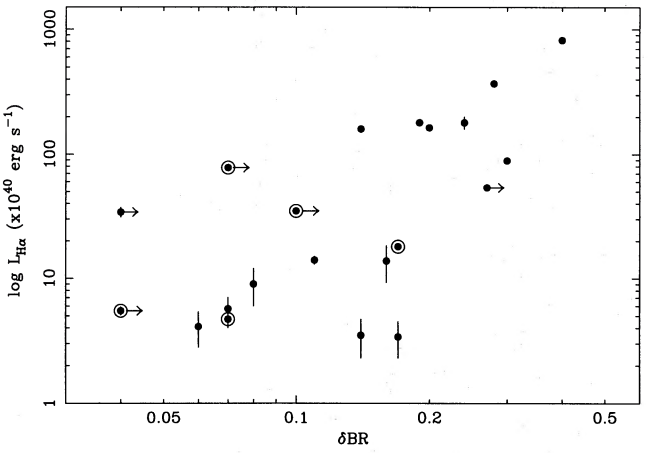

Figure 5. The variation in the measured Hα luminosity with δBR. Ringed points are the lowest redshift galaxies, where it is expected that the measured Hα luminosity is an underestimate due to limited slit coverage. Galaxies that were not observed close to the parallactic angle ($>30°$) are marked as lower limits to the δBR.

shift sources are predominately at lower galactic latitude (four out of six have $|b|$ of 20° to 30°), and so many have been missed by Abell through increased star density and/or Galactic obscuration. These clusters are similar to the two non-optically classified clusters in the ESF sample (2A0335+096 and Hydra A) and are a few per cent of the overall sample. The similarity also applies to the radio and X-ray properties, with the rate of radio detection and the high fraction of cooling flows in the new members of the BCS from our initial *ROSAT* pointed observations matching the original sample of the 50 brightest clusters (ESF).

There is clearly some link between the radio and optical properties of the clusters, as the fraction of line-emitting systems ($W_{H\alpha} > 2$ Å) with a radio detection in our sample is higher (33 per cent for any power, and 21 per cent for $P_{1.4} > 25$) than those without (16 and 11 per cent, respectively). As noted above, the detection rate for $P_{1.4} > 25$ is a lower limit, as a number of the more distant clusters have upper limits above $P_{1.4} = 25$. These fractions are consistent with the ESF sample where, although every line-emitting system has a radio source of some power (some of log powers of 22–23), only 35 per cent of the line emitters and 13 per cent of the non-line emitters have $P_{1.4} > 25$. Whilst it is clear that the presence of a central radio source increases the probability of line emission and blue light, there is no detailed correlation found – there are systems with substantial radio emission and no line emission (e.g. A2029), and systems with powerful line emission and only a faint radio source (e.g. A1068 and 2A0335+096). To investigate this point further, we have taken the line-emitting galaxies from our sample and those of Donahue et al. (1992), and plotted line luminosity against radio power (Fig. 6). The EMSS sources have significantly more accurate radio fluxes than the BCS sources, as VLA snapshots were made of all EMSS sources and are presented in Stocke et al. (1991). The EMSS clusters fill the full range of radio power, illustrating the lack of any correlation. The important advance made by the EMSS and BCS is that they are X-ray-selected and hence are not biased towards central galaxies containing powerful radio sources, unlike the Heckman et al. (1989) sample which was chosen to include the most luminous radio sources. Radio-selection results in a bias to higher radio luminosity for the powerful line emitters and hence an apparent correlation, even though line emitters of low Hα luminosity (10^{40} erg s^{-1}) show a range of radio luminosity of a factor of 10^3. This effect may have important implications for the observed correlation between line luminosity and radio power for radio galaxies (see Rawlings & Saunders 1991).

As all the clusters contained in this paper and Paper I are selected to be the X-ray-bright, it is also probable that they

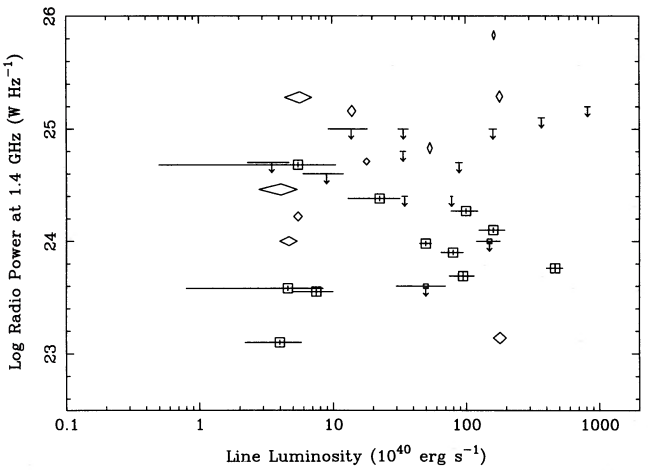

Figure 6. The variation of radio power at 1.4 GHz and optical line luminosity fr the BCS and EMSS samples. The diamonds and upper limits are from the BCS (Paper I and this paper), and the squares are from the EMSS (Stocke et al. 1991; Donahue et al. 1992).

are the most luminous due to evolution (Edge et al. 1990; Gioia et al. 1990b). Subcluster merging activity is thus also a likely source of energy input to drive the shocks powering the most luminous nebulae, or to trigger a fading starburst. The entire BCS will enable us to sample a wide redshift range to test for any match between subcluster merging activity and the optical properties of the galaxy.

ACKNOWLEDGMENTS

The Isaac Newton Group of Telescopes at the Observatorio del Roque de los Muchachos del Instituto de Astrofísica de Canarias is operated by the Royal Greenwich Observatory on behalf of the Science and Engineering Research Council (UK). The NASA/IPAC Extragalactic Database is operated by the Jet Propulsion Laboratory, California Institute of Technology (USA) under contract with NASA. ACF thanks the Royal Society for financial support, and CSC acknowledges the support of a Post-doctoral Fellowship from the Science and Engineering Research Council.

REFERENCES

Abell G. O., 1958, ApJS, 3, 211
Allen S. W. et al., 1992, MNRAS, 259, 67 (Paper I)
Arnaud M., Lachieze-Rey M., Rothenflug R., Yamashita K., Hatsukade I., 1991, A&A, 243, 56
Ball R., Burns J. O., Lokern C., 1993, AJ, 105, 53
Brandt W. N., Fabian A. C., Nandra K., Reynolds C. S., Brinkmann W., 1994, MNRAS, 271, 958
Cowie L. L., Hu E. M., Jenkins E. B., York D. G., 1983, ApJ, 272, 29
Crawford C. S., Fabian A. C., 1992, MNRAS, 259, 265
Crawford C. S., Fabian A. C., 1993, MNRAS, 265, 431
Donahue M., Stocke J. T., Gioia I. M., 1992, ApJ, 385, 49
Ebeling H., Böhringer H., Voges W. H., Edge A. C., 1993, A&A, 275, 360
Edge A. C., Stewart G. C., Fabian A. C., Arnaud K. A., 1990, MNRAS, 45, 559
Edge A. C., Stewart G. C., Fabian A. C., 1992, MNRAS, 258, 177 (ESF)
Edge A. C., Fabian A. C., Allen S. W., Crawford C. S., White D. A., Böhringer H., Voges W. H., 1994, MNRAS, 270, L1
Gioia I. M., Maccacaro T., Schild R. E., Wolter A., Stocke J. T., Morris S. L., Henry J. P., 1990a, ApJS, 72, 567
Gioia I. M., Henry J. P., Maccacaro T., Morris S. L., Stocke J. T., Wolter A., 1990b, ApJ, 356, L35
Heckman T. M., Baum S. A., van Breugel W. J. M., McCarthy P., 1989, ApJ, 338, 48
Henry J. P., Gioia I. M., Maccacaro T., Morris S. L., Stocke J. T., Wolter A., 1992, ApJ, 386, 408
Hu E. M., Cowie L. L., Wang Z., 1985, ApJS, 59, 447
Johnson M. W., Cruddace R. G., Ulmer M. P., Kowalski M. P., Wood K. S., 1983, ApJ, 266, 425
Johnstone R. M., Fabian A. C., Nulsen P. E. J., 1987, MNRAS, 224, 75
Kurucz K. L., 1979, ApJS, 40, 1
Lucey J. R., 1983, MNRAS, 204, 33
McNamara B. R., O'Connell R. W., 1989, AJ, 98, 2018
McNamara B. R., O'Connell R. W., 1993, AJ, 105, 417
Nesci R., Gioia I. M., Maccacaro T., Morris S. L., Perola G. C., Schild R. E., Wolter A., 1989, ApJ, 344, 104
Owen F. N., White R. A., Hildrup K. C., Hanish R. J., 1982, AJ, 87, 1983
Pesce J. E., Fabian A. C., Edge A. C., Johnstone R. M., 1990, MNRAS, 244, 58
Rawlings S., Saunders R., 1991, Nat, 349, 138
Romanishin W., 1987, ApJ, 323, L133
Romanishin W., 1988, in Fabian A. C., ed., Cooling Flows in Clusters and GAlaxies. Reidel, Dordrecht, p. 121
Stocke J. T., Morris S. L., Fleming T. A., Gioia I. M., Maccacaro T., Schild R., Wolter A., Henry J. P., 1991, ApJS, 76, 813
Voges W. et al., 1992, in Guyenne T. D., Hunt J. J., eds, Proc. Satellite Symp. 3, ESA ISY-3, p. 223
White R. L., Becker R. H., 1992, ApJS, 79, 331